TRW

ER-6356

FACILITY FORM 602

N65 18131 (ACCESSION NUMBER) (THRU)

34 (PAGES) 1 (CODE)

CR-57102 (NASA CR OR TMX OR AD NUMBER) 03 (CATEGORY)

BRAYTON CYCLE CAVITY RECEIVER DEVELOPMENT

QUARTERLY REPORT

GPO PRICE $ _____

OTS PRICE(S) $ _____

Hard copy (HC) $2.00

Microfiche (MF) $0.50

TRW ELECTROMECHANICAL DIVISION

THOMPSON RAMO WOOLDRIDGE INC.

23555 EUCLID AVENUE ■ CLEVELAND, OHIO 44117

OCTOBER 1964 — DECEMBER 1964

ER-6356

BRAYTON CYCLE CAVITY

RECEIVER DEVELOPMENT

QUARTERLY REPORT

Technical Management
NASA-Lewis Research Center
Solar and Chemical Power Branch
Attn.: J. A. Milko (86-1)

TRW ELECTROMECHANICAL DIVISION
Thompson Ramo Wooldridge Inc.
Cleveland, Ohio

OCTOBER 1964 - DECEMBER 1964

TABLE OF CONTENTS

1.0 PROJECT OBJECTIVES

The Brayton cycle cavity receiver development program as presently planned consists of three phases. Phase I is being performed currently and features both a design study of the full-scale flightweight unit and a material compatibility investigation with lithium fluoride as the corrosive salt. Phase II is contemplated to consist of construction and ground test of the flightweight unit. Phase III is planned as the endurance test of the flightweight unit. The ultimate objective of the program is to demonstrate a one year endurance capability of the flightweight unit in a ground test.

2.0 PROJECT OBJECTIVES FOR THE REPORTING PERIOD OF OCTOBER 1, 1964 THROUGH DECEMBER 31, 1964 (REPEATED FROM THE PREVIOUS QUARTERLY REPORT)

1. Continued examination of the failures encountered in Task II.
2. Continuation of furnace test no. 1 in Task III.
3. Initiation of furnace test no. 2 in Task III.
4. Continuation of the small scale experiments under Amendment 4.
5. Completion of the two percent gas pressure drop cavity receiver design layout under Task IV.
6. Continuation of the cavity temperature distribution calculations under Task IV.
7. Completion of the aperture control design analysis under Task IV.

3.0 PROJECT PROGRESS DURING THE REPORTING PERIOD

3.1 Task II Progress

All testing on Task II was completed in July, 1964, but the analysis of the corrosion test capsules continued during the quarter. Results of the metallographic examination of the selected test capsules were reported in the last quarterly progress report, ER-6102, and typical photomicrographs shown. As reported therein, four capsule specimens taken from previously failed capsules were submitted for electron microprobe analysis. The results of the electron microprobe analysis were listed in Table III of ER-6102. At that time, it was felt that additional information was required to identify more clearly the cause of the composition changes. Hence, three additional specimens were submitted for electron microprobe analysis. These specimens were taken from TD Nickel Capsule No. 19, Hastelloy X Capsule No. 24 and Waspaloy Capsule No. 28. The results of the electron microprobe analysis on these three specimens are discussed below.

TD Nickel Capsule No. 19 Section No. 2

Previous metallographic examination revealed light depletion to a depth of 3-1/2 mils. Also, as shown in Figure 1, there was evidence of grain recrystallization along the surface to a maximum depth of 1-1/2 mils. The results of the microprobe analysis revealed essentially a complete loss of thorium and an increase in nickel content in the 1-1/2 mil wide recrystallized band. No compositional differences in nickel and thorium were found in the 2 mil wide depleted band beneath the recrystallized band.

During the analysis, a visible violet fluorescence was noted in the TD nickel matrix. This fluorescence is a result of electron excitation of the ThO_2. In the recrystallization band, no fluorescence was noted where the depletion of the thorium occurred. And in the band where the light depletion occurred, the fluorescence was greatly diminished, whereas the thorium content was the same as the matrix. From these results, it appears that the ThO_2 in the depleted band was decomposing to thorium dissolved in a nickel matrix. The recrystallized band is likely the result of the absence of dispersed ThO_2 which hinders grain growth.

Hastelloy X Capsule No. 24 Section No. 3

Previous metallographic examination revealed a light depletion to a maximum depth of 2 mils as shown in Figure 2. Also, in the unetched condition, a second phase was noted along the grain boundaries. Upon etching, this phase tended to over-etch as evidenced in Figure 2. The results of microprobe analysis revealed no significant variation in chemistry throughout the specimen. However, the grain boundary precipitate was found to be slightly enriched in molybdenum. No further identification of this phase was attempted.

Waspaloy Capsule 28 Section No. 3

Previous examination of the specimen revealed attack in the form of leaching (Zone 1) and depletion (Zone 2) to a maximum depth of 5 mils as shown in Figure 3. In Zone 2, the nickel content dropped from 56 w/o to 55 w/o and in Zone 1, dropped to essentially a constant value of 52 w/o. This distribution is shown in Figure 4. The chromium content appeared to increase slightly in Zone 2 from a matrix value of 19.5 w/o to 21.1 w/o at the start of Zone 1. In Zone 2, the chromium content dropped back to 19.5 w/o and then rose to a value of 22.6 w/o right at the edge. A decrease in titanium was found in Zone 2 from a matrix value of 3.0 w/o to 1/5 w/o. At the start of Zone 1, the titanium rose to 8 to 10 w/o and then dropped off to 3.5 w/o at the edge.

No changes in iron, molybdenum, cobalt and aluminum were found in Zone 2. However, in Zone 1 the iron increased from 1.0 w/o to 1.4 w/o, the molybdenum from 4.3 w/o to 5/1 w/o, the cobalt dropped from 13.5 w/o to 12.5 w/o, and the aluminum dropped from 1.3 to 1.0 w/o.

From the results it appears that nickel, cobalt, and aluminum were removed from the Waspaloy. However, the reason for the variations in chromium and titanium contents are not definite at this time.

3.2 Task III Progress

During the quarterly reporting period, the test in furnace #1 was continued and the test in furnace #2 started, as shown in the project schedule for Task III, Figure 5. Three interruptions occurred in the furnace #1 test. At 2111 hours on November 5, furnace #1 was shut down by an open thermocouple on the over-temperature protection controller. The thermocouple was replaced and the furnace restarted at 1055 on November 11. At 1000 hours on December 2, a white vapor was noticed coming from the argon bubbler. The electrical conductivity of the solution in the bubbler was rising also. The conductivity rise was verified with a new solution, and the furnace was shut down at 1500 on December 2. The furnace had accumulated 2003 hours of test operation.

The capsule test container was opened and the capsules removed. The capsules were then examined by visual, die-penetrant and radiographic methods. On the basis of this examination, Waspaloy Capsule No. 27 was removed from the test, for it was the only capsule in which the presence of lithium fluoride could not be detected in the radiographs. Also, dye-penetrant inspection of the capsule revealed a small longitudinal crack in the middle of one of the longitudinal seam welds.

The remaining capsules were reinstalled in a new test container and mounted in the furnace. The test was re-started at 0840 on December 14. During the remainder of the quarter, the furnace operated normally. However, 6 hours of operating time were lost because of a broken Globar heating element. As of midnight December 31, the furnace had accumulated 2401 hours of operation. The heating portion averaged 1.32 hours/cycle and the cooling portion averaged 0.51 hours/cycle.

The capsules which were tested in Task II for 4661 hours had 7062 hours of test time as of midnight December 31. The Hastelloy N Capsule which had 3989 hours in Task II had been exposed to 6390 hours of test time as of midnight December 31.

The testing in furnace #2 was started at 1030 on November 11. It has been interrupted several times because of equipment failures. The furnace lost a total operating time of 51 hours caused by these failures. As of midnight December 31, the furnace had

accumulated 1031 hours of operation. The cooling part of the cycle averaged 0.75 hour/cycle, and the heating averaged 1.03 hours/cycle.

Examination of the Waspaloy Capsule No. 27 removed from furnace #1 has been partially completed. Metallographic examination of sections removed from the capsule have revealed corrosive attack in the form of pitting and leaching to a maximum depth of 4 mils. The capsule failure was located in the weld bead, but the exact spot of the failure could not be located in the metallographic specimens. This capsule had operated for 5,992 hours. The heating portion averaged 1.09 hours/cycle, and the cooling averaged 0.50 hour/cycle.

3.3 Amendment No. 4 Progress

The objective of the work effort specified in Amendment 4 is to provide additional data on the heat input and heat release characteristics of lithium fluoride. Seven additional modules are to be constructed and tested as listed in Table I below.

TABLE I AMENDMENT 4 MODULES

Module No.	Purpose	Status
A	Heat Input - Bare	Testing Complete
B	Heat Input - Fins	Testing Complete
C	Heat Input - Fins	Testing Complete
Dummy 1	Heat Release - Freeze Pattern	Testing Complete
Dummy 2	Heat Release - Test Technique	Ready for Test
D	Heat Input and Release - Bare	In Fabrication
E	Heat Input and Release - Fins	In Fabrication

The basic material of construction for all modules is Haynes Alloy 25. The fins are commercial Grade A Nickel in all cases. The coolant tubes in the dummy modules and Modules D and E are 316 stainless steel.

The two dummy modules are being tested to develop new test techniques in which the fluoride is frozen in a controlled pattern around each successive coolant tube. A secondary objective of the dummy tests is to demonstrate that the new techniques do in fact provide the desired freeze patterns. The project schedule for the Amendment 4 work effort is shown in Figure 6.

The test results for Module A are shown in Figure 7. Similar results for Modules B and C are given in Figures 8 and 9, respectively. Finally, the results for all three modules at a constant coolant flow rate are included in Figure 10. The analytical results obtained from an analog solution described later are also presented for comparison in Figures 7, 8 and 9.

Results from an initial test of Module A were very close to those shown for Module B in Figure 8. In view of this situation, a second set of tests were conducted on Module A. Prior to the second round of tests, all of the lithium fluoride was removed, the module was cleaned chemically, rinsed and dried. A new charge of lithium fluoride was subsequently loaded into Module A and testing initiated. The test results indicated for Module A in Figure 7 are those obtained from the second test. The results exhibited a reduced spread in the data compared to the first test, but no significant difference was noted.

An analytical investigation was conducted to determine mathematical expressions for the heat transfer from a hot surface, such as the module top plate, to the fluoride storage bath under conditions of melting or freezing, indicated by a moving fusion front. Because the location of the moving boundary (the melt line) is unknown, the problem is non-linear, and exact analytical techniques for solving this type of problem are not available at present. Therefore, recourse was taken to examination of approximate methods, including finite differences, variational principles and heat balance integrals. The heat balance integral method was selected as the most

convenient in this application, and expressions were subsequently derived which present the heat transfer in the form of an integro-differential equation. This equation can be solved either by the use of Laplace transforms or a differential analog computer.

A review of the manpower effort required to solve the problem by purely analytical means indicated that it would be a formidable task and could be accomplished with much less effort and at a much lower cost by an analog solution. Therefore, an analog solution was completed, and the results for the bottom surface of the top plate, analogous to a thin-shell cavity surface, are shown in Figure 11. The analog results given previously in Figure 9 indicate reasonable agreement between the analytical predictions and the experimental data.

The first dummy module, which has the same internal bath configuration as Module D, was loaded with fluoride and tested. As of December 31, 1964, the testing of this module was completed and the module ready for examination.

3.4 Task IV Progress

The Task IV work effort consists of three parts:

1. Two percent allowable gas pressure drop full scale cavity receiver design.
2. Aperture control analysis
3. Cavity temperature distribution.

Each of these parts will be discussed in order. The revised project schedule for Task IV is shown in Figure 12.

3.4.1 Two Percent Pressure Drop Design

As noted in the last quarterly progress report, ER-6102, the initial design featured 70 tubes and a mean gas Reynolds number of about 5500. It was discovered at that time that the tube curvature was sufficient to cause doubt on the flow regime at this Reynolds number. Independent evidence indicated the flow could be on the borderline between transitional and turbulent flow. This situation was undesirable because it

could cause erratic heater operation. Accordingly, a second design was initiated and the basic tube layout was in progress at the time of publication of ER-6102. This design features a mean gas Reynolds number of about 8100 with 30 tubes of 1.050 inches inner diameter 118.3 inches long.

Examination and review of the resultant internal bath configuration indicated that this design was acceptable and in fact was more favorable than the initial design. To determine if this trend would continue, a third design was investigated at a mean gas Reynolds number of about 10,000. This design employed 20 tubes, but the review of this one showed no additional advantages above the 30 tube design. The void volume in the 20 tube design was significantly greater than that in the 30 tube design. The added void volume was considered a disadvantage, and therefore, the 30 tube design was rated the best of the three and near optimum. Therefore, the 30 tube design layout was completed, and is shown in Figure 13.

The stress analysis conducted on the full scale cavity receiver design was confined to the 30-tube model. The areas examined included the following:

1. Inner shell - buckling and membrane stresses
2. Outer shell - buckling and membrane stresses
3. Outer shell - to - outlet header joint
4. Outer shell - to - inlet header joint
5. Inner shell - to - inlet header joint
6. Tube membrane and thermal stresses
7. Inlet and outlet header membrane stresses
8. Aperture control mechanisms.

The inner and outer shells were approximately by cones and cylinders. The thermal stresses were based on temperature conditions assumed from earlier results on the Sunflower boiler/heat storage program. These temperature assumptions were made on the high side for conservative design. The maximum inner shell temperature was set at 1750°F with the range down to 1650°F, locally.

The results showed that the outlet header pseudo-shell needed to be much thicker, approximately 1/4-inch, and that the outer shell near the outlet header should be 0.080-inch thick for a short distance from the header joint and a gradual taper to the basic shell minimum thickness of 0.050-inch. Considerable study of the conditions at the inner shell-to-inlet header joint resulted in a recommendation to move the aperture cone and, therefore, the solar concentrated incident energy, to a position three inches from the header in lieu of the present position two inches from the header.

The tube stresses are very low and of no consequence. The inlet and outlet header wall thicknesses must be based on long-term steady stress levels. The inlet header must be integrated with the NASA mounting ring design. It would be desirable to determine all the resultant stresses on the STL shell and ring computer.

In November, the NASA cognizant technical personnel requested a discussion and review of the potential heat transfer and pressure drop correlations for design of the heater. Several technical meetings were held between TRW and NASA personnel in an effort to reach agreement on the correlations that should be employed in the heater design.

After considerable review by both TRW and NASA, an agreement was finally achieved to employ a particular pair of correlations in the heater design. The heater designs made to date by TRW have not employed these correlations. Since the time of this agreement, the influence of the use of these correlations for the heater design on the overall cavity receiver design has been examined by TRW. This examination is still in process.

3.4.2 Aperture Control Analysis

The mechanisms necessary for the two systems required on the aperture cone assembly were analyzed and designed. The systems are the aperture closure doors to retain cavity heat during shade time and the heat rejection doors to limit the cavity surface temperature during orbits where all-sun conditions are encountered.

Following a technical review of the program conducted at NASA early in December, NASA has directed that the aperture closure doors are to be removed and additional heat rejection capability provided. A schematic view illustrating both systems is shown in Figure 14. It is to be understood that the aperture closure doors will be removed, and a new layout made.

The basic ingredients for the heat rejection system include heat sensors on the cavity surface, a liquid metal working fluid, actuating bellows on the aperture cone, and hinge-mounted louvers. The liquid metal is boiled at the desired control temperature in the sensors. The associated vapor pressure is transmitted through the loop to the bellows which actuate the louvers. A spring return is provided to obtain fail-safe operation with the louvers in the closed position.

The design analysis for the two systems was completed on schedule.

3.4.3 Cavity Temperature Distribution

The general objective of this work effort is to determine cavity temperature distributions for several conditions of collector misorientation and cavity surface emissivity for the receiver design shown in Figure 13.

The task involves the integration of solar collector characteristics with the receiver design to predict steady state performance of the system. To be taken into consideration is the heat storage capacity of the lithium fluoride material and the variable resistance to heat transfer resulting in the lithium fluoride bath during the heat addition process. On this basis, a quasi-transient solution is obtained by determining the steady state solution at finite periods of time in the period of the orbit. The general problem is shown schematically in Figure 15. The simplified schematic illustrates the action of the inner loop to define surface temperature distribution for fixed resistances to heat transfer in the lithium fluoride heat storage bath and gas heat exchanger. The procedure involves the successive iteration of cavity surface temperature to satisfy the cavity and the heat storage, heat exchanger subroutine requirements. The input data includes the incident solar flux distribution on the cavity surface as determined in Reference 1 for

the conditions of solar collector misorientation of 0, 15 and 30 minutes of arc. In the outer loop, the movement of the melt line in a finite time is determined by means of electric analog techniques to define new thermal resistance values in the heat storage bath and heat exchange for the subsequent time increment.

In the reporting period, the interfaces between all subroutines of the main computer program have been defined, subroutine flow diagrams prepared and programming initiated for most. The cavity subroutine, which respresents a major element in the main program is currently in the advance stages of programming and checkout. This subroutine consists of three main parts, an interpolation procedure, the solar part which treats only the solar component of energy and the thermal part which takes into account the energy exchange within the cavity due to thermal radiation. The interpolation procedure functions to take the basic output data of Reference 1, to provide a finer interpolation of flux distribution on the cavity surface. This procedure is complete and fully checked out. The solar portion of the subroutine has also been programmed and is in the advanced stages of checkout. Upon its completion the effort of programming and checkout of the thermal part will be initiated.

In the electric analog simulation of the heat addition process, basic correlations have been obtained relating the various thermal resistances of the heat storage media to the melt line position. The heat addition process is shown schematically in Figure 16. The figure illustrates a typical position of the melt line in contact with the tube wall at some time after initiation of heat addition.

In the electrical analog, the film resistance of the gas is simulated by an equivalent electrical resistance such that voltage differential between the cavity wall and tube is proportional to the temperature difference. Similarly, by inserting the resistance r, the voltage difference between the cavity wall and melt line becomes proportional to the actual temperature differential. With the potentiometer and microammeter, lines of constant potential can be located in the liquid and solid regions. Once the equal potential lines have been defined, the local movement of the melt line in a finite time increment is defined by the equation

$$(g_s)_m - (g_m)_g = H \frac{\Delta S \ \Delta M}{\Delta t} \rho$$

where, ΔM is the local movement of the melt line perpendicular to the differential section ΔS.

H is the heat of fusion of LiF

ρ is the density of solid LiF

Δt is the time increment

and $(g_s)_m$ and $(g_m)_g$ are proportional to $(i_s)_m$ and $(i_m)_g$ respectively.

The results of the measurements made on the electric analog are illustrated in Figure 17 for a tube section near the inlet. The geometrical resistance values are plotted as a function of percentage liquid volume. In the simulation the cavity wall temperature is assumed constant at 1580°F corresponding to the melt temperature of lithium fluoride. This is considered to be valid since during the process of heat of fusion addition, the local temperature of the cavity wall is not expected to change too greatly due to the relatively high thermal conductivity of the liquid fluoride in combination with the constant temperature heat storage capacity of the fluoride. At the time of complete utilization of the heat of fusion of the fluoride, the local surface temperature can be expected to rise rapidly due to the excess energy available.

List of References

Reference 1 - Schrenk, G. L., "Solar Collection Limitations for Dynamic Converters," Paper presented at the Sixth AGARD Combustion and Propulsion Colloquim, Cannes, France, March 1964.

4.0 CURRENT PROBLEM AREAS

The current problem areas are schedule slippages in two tasks

1. Amendment #4 - The module testing continues to be about 2 weeks behind schedule.
2. Task IV - The state-of-the-art extensions required in the cavity temperature distribution effort needed more manpower and time than was negotiated. Therefore, this effort is about 10 weeks behind the negotiated schedule.

5.0 PLANNED DIRECTION OF EFFORT FOR THE NEXT QUARTER

During the next quarter, the effort will be directed toward the following:

1. Continuation of furnace test No. 1 on Task III
2. Continuation of furnace test No. 2 on Task III
3. Completion of all work in Amendment 4
4. Completion of all work in Task IV

Figure 1. Photomicrograph of Section No. 2 from TD Nickel Capsule No. 19 Showing the Attack Incurred after 4661 Hours Exposure to LiF.
Etchant: 10% Ammonium Persulfate; 10% Potassium Cyanide
250 x

Figure 2. Photomicrograph of Section No. 2 from Hastelloy X Capsule No. 24 Showing the Light Depletion Incurred after 4661 Hours Exposure to LiF.
Etchant: Electrolytic - 10% Oxalic
250 x

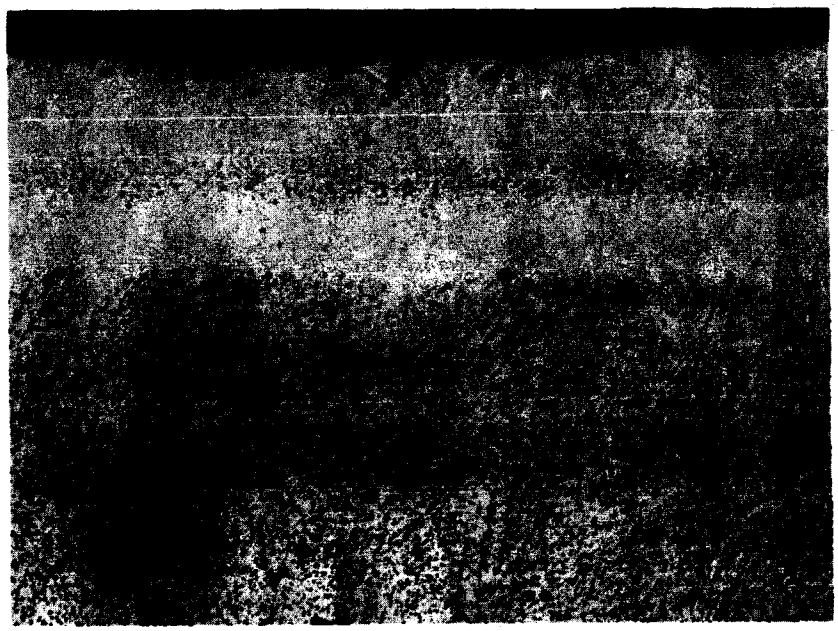

Figure 3. Photomicrograph of Section No. 3 from Waspaloy Capsule No. 28 Showing the Combined Leaching and Depletion Attack Incurred after 3989 Hours Exposure to LiF.
Etchant: $HF-HNO_3-H_2SO_4-H_2O$

250 x

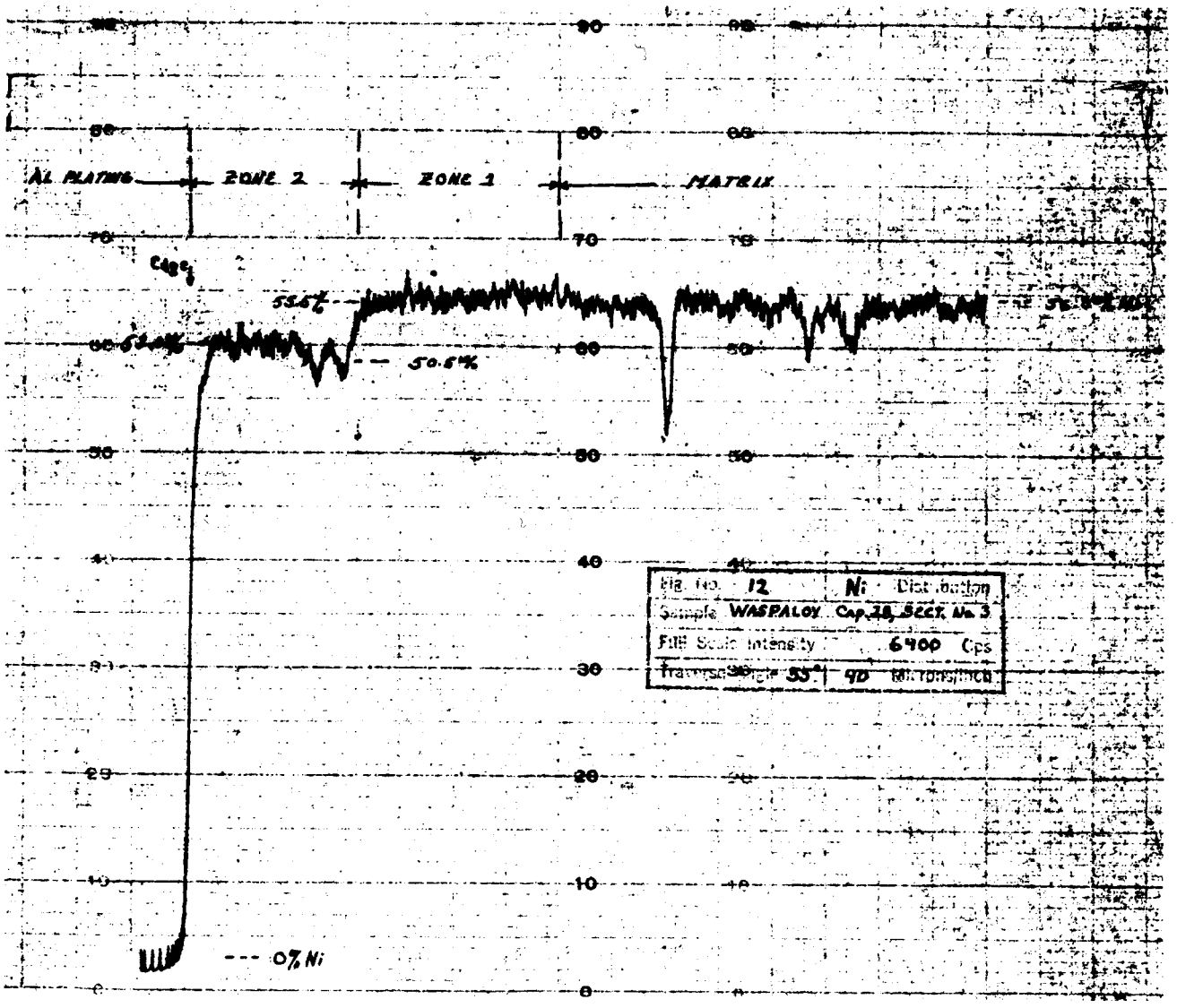

Figure 4. Chart of the Microprobe Trace for Nickel in Section No. 3 from Waspaloy Capsule No. 28.

PROJECT SCHEDULE, TASK III, ADDITIONAL CORROSION TESTING

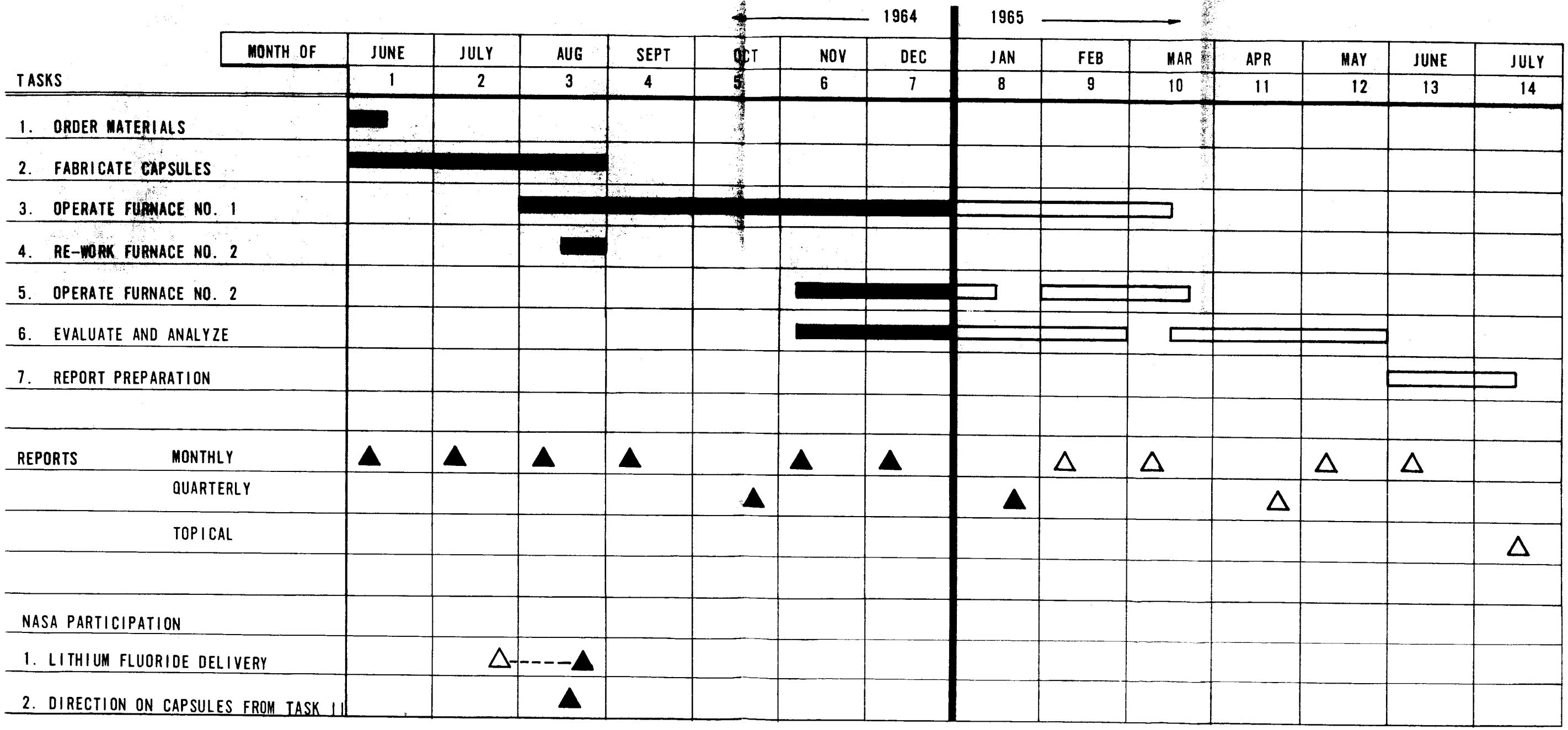

FIGURE 5

PROPOSED SCHEDULE

PROJECT SCHEDULE FOR AMENDMENT NO. 4 TO CONTRACT NAS 3-2779

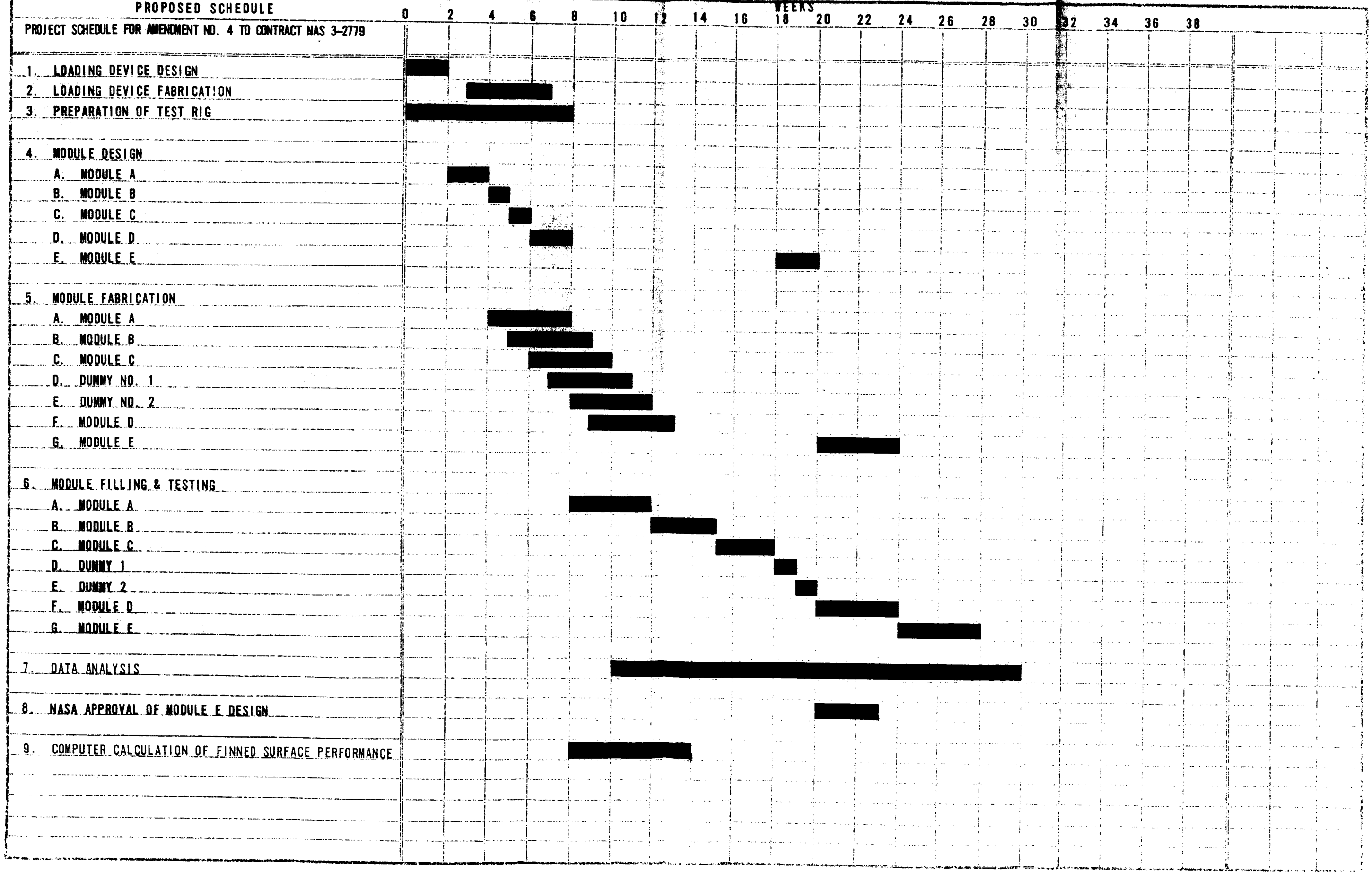

FIGURE 6

VARIATIONS OF MAXIMUM TOP PLATE TEMPERATURE WITH HEAT INPUT FLUX LEVEL

MODULE "A"

(TEMPERATURES UNCORRECTED FOR TOP PLATE ΔT)

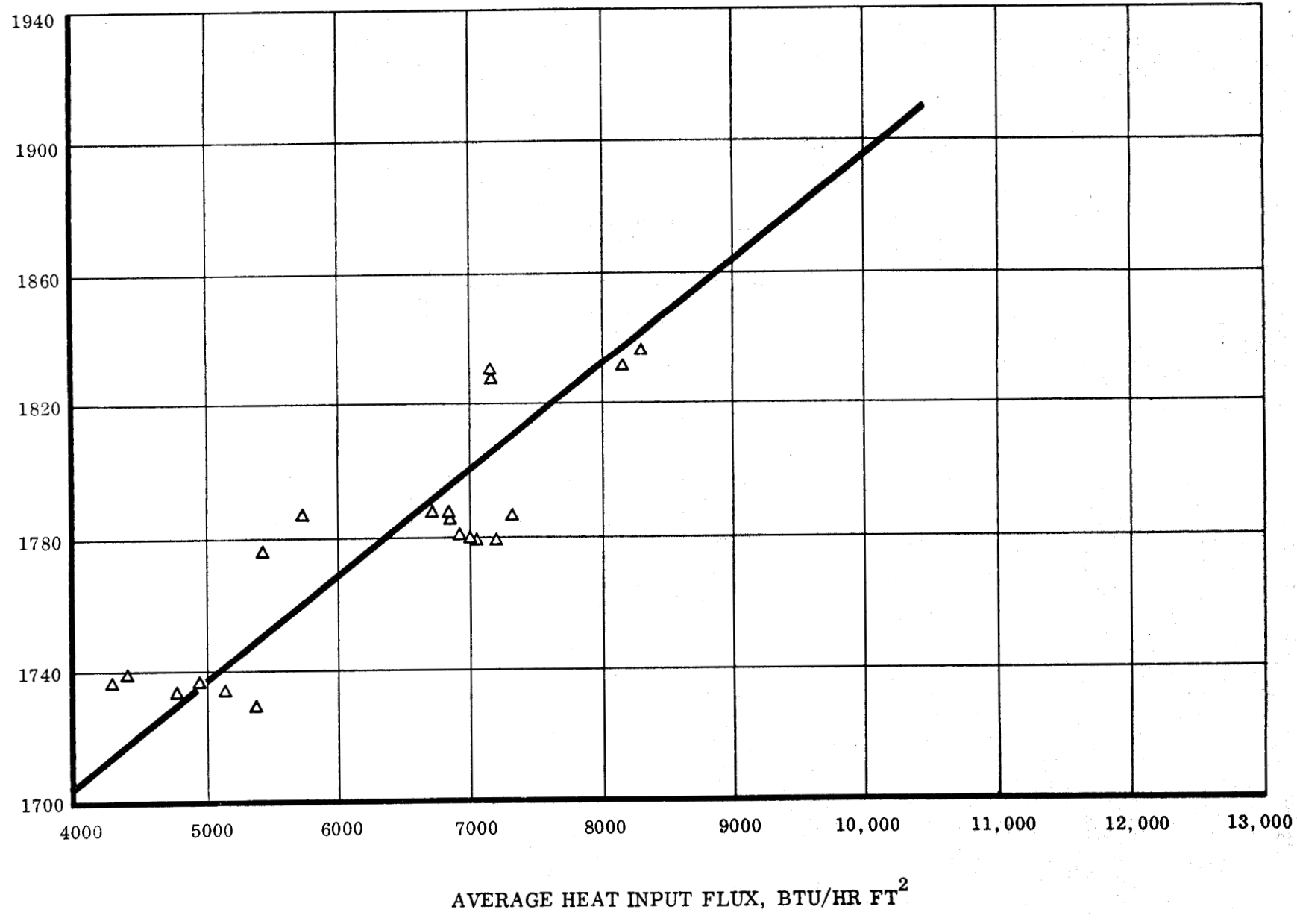

FIGURE 7

TRW ELECTROMECHANICAL DIVISION
THOMPSON RAMO WOOLDRIDGE INC.

VARIATION OF MAXIMUM TOP PLATE TEMPERATURE WITH HEAT INPUT FLUX LEVEL

(MODULE "B")

(TEMPERATURES UNCORRECTED FOR TOP PLATE ΔT)

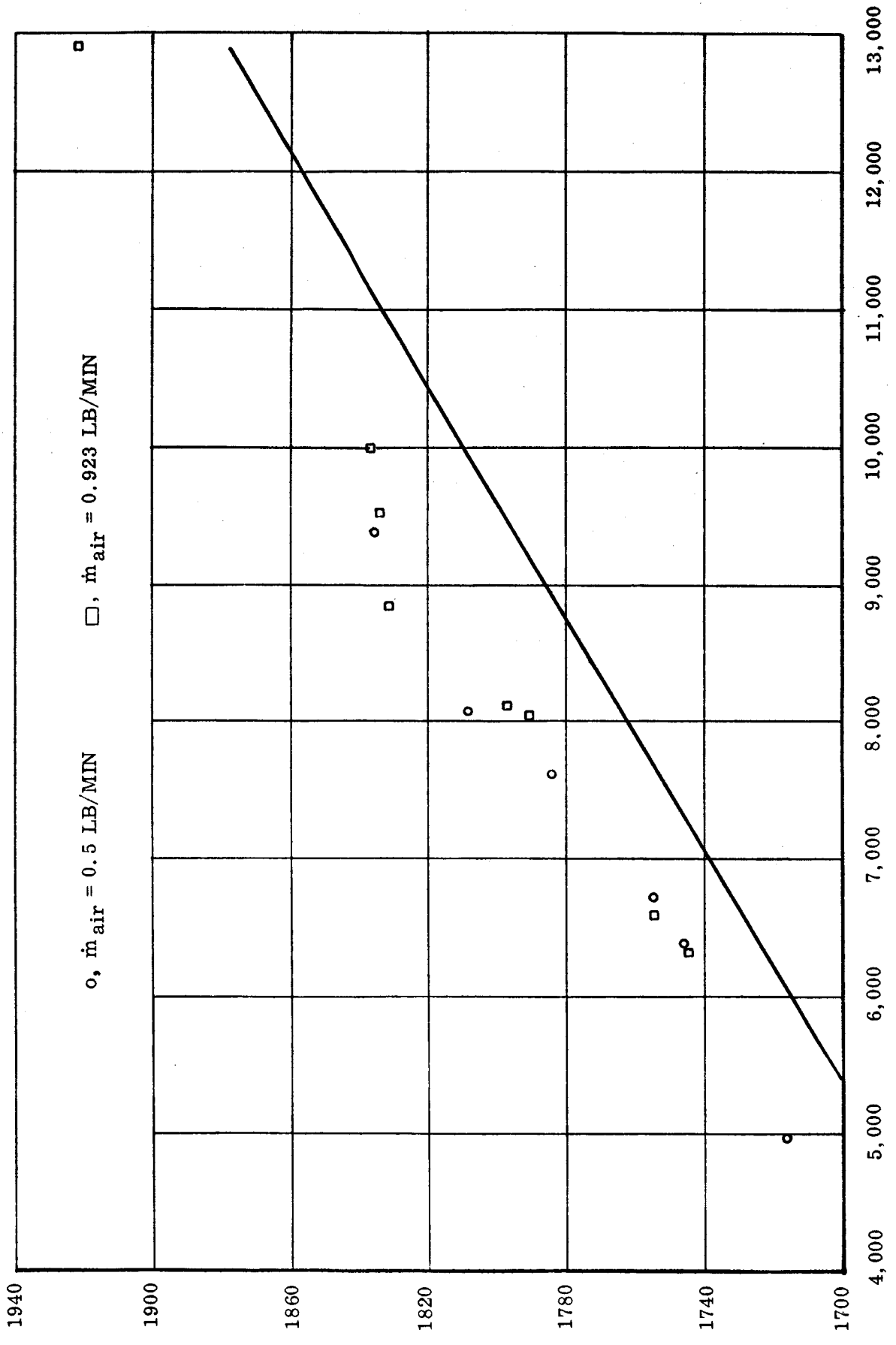

FIGURE 8

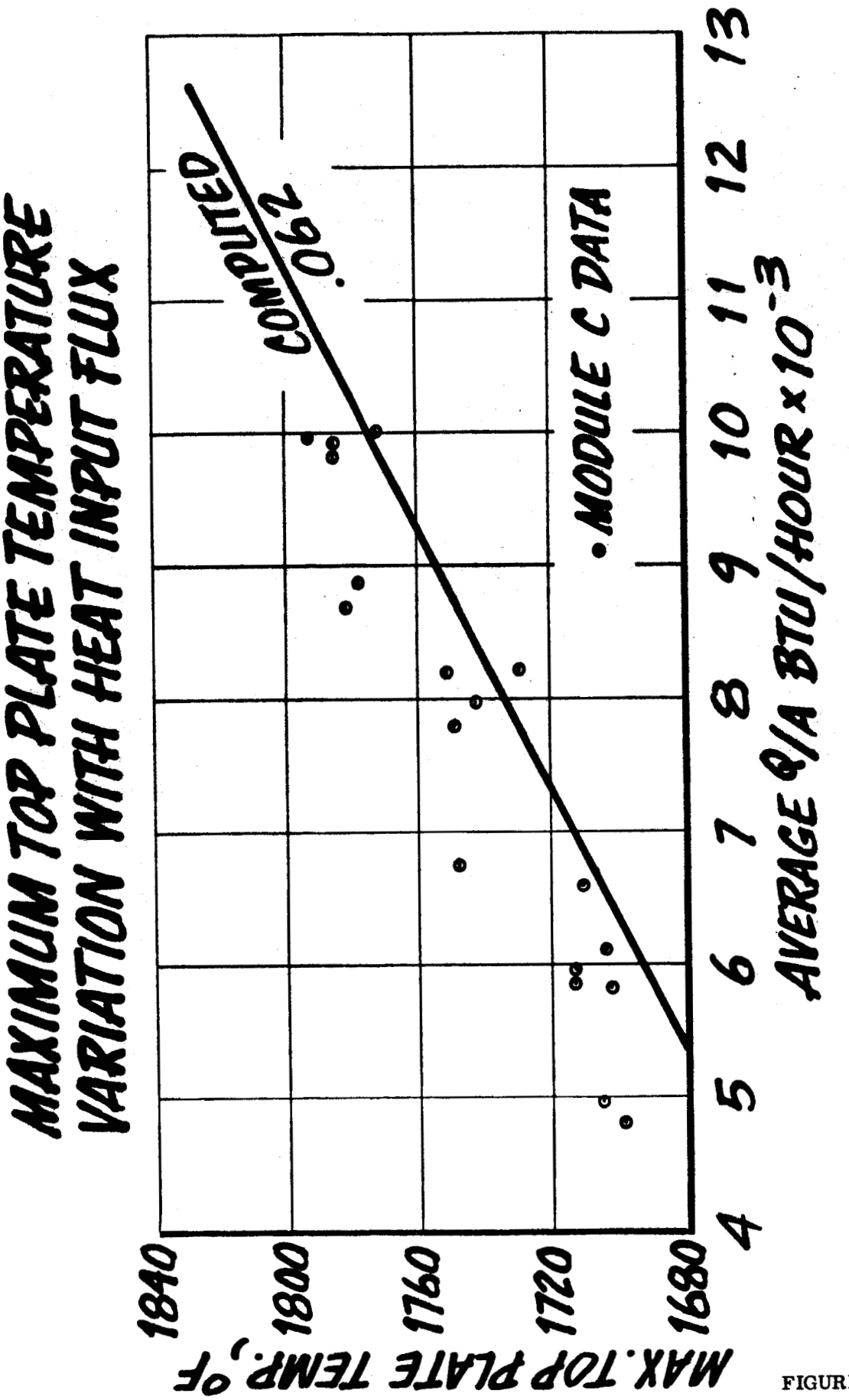
MAXIMUM TOP PLATE TEMPERATURE
VARIATION WITH HEAT INPUT FLUX
COMPUTED
.062
• MODULE C DATA
MAX. TOP PLATE TEMP., °F
1840
1800
1760
1720
1680
4
5
6
7
8
9
10
11
12
13
AVERAGE Q/A BTU/HOUR x 10⁻³

FIGURE 9

VARIATION OF MAXIMUM FOR PLATE TEMPERATURE WITH HEAT INPUT FLUX LEVEL
FOR MODULES A, B AND C AT A CONSTANT COOLANT FLOW OF 0.5 LB/MIN

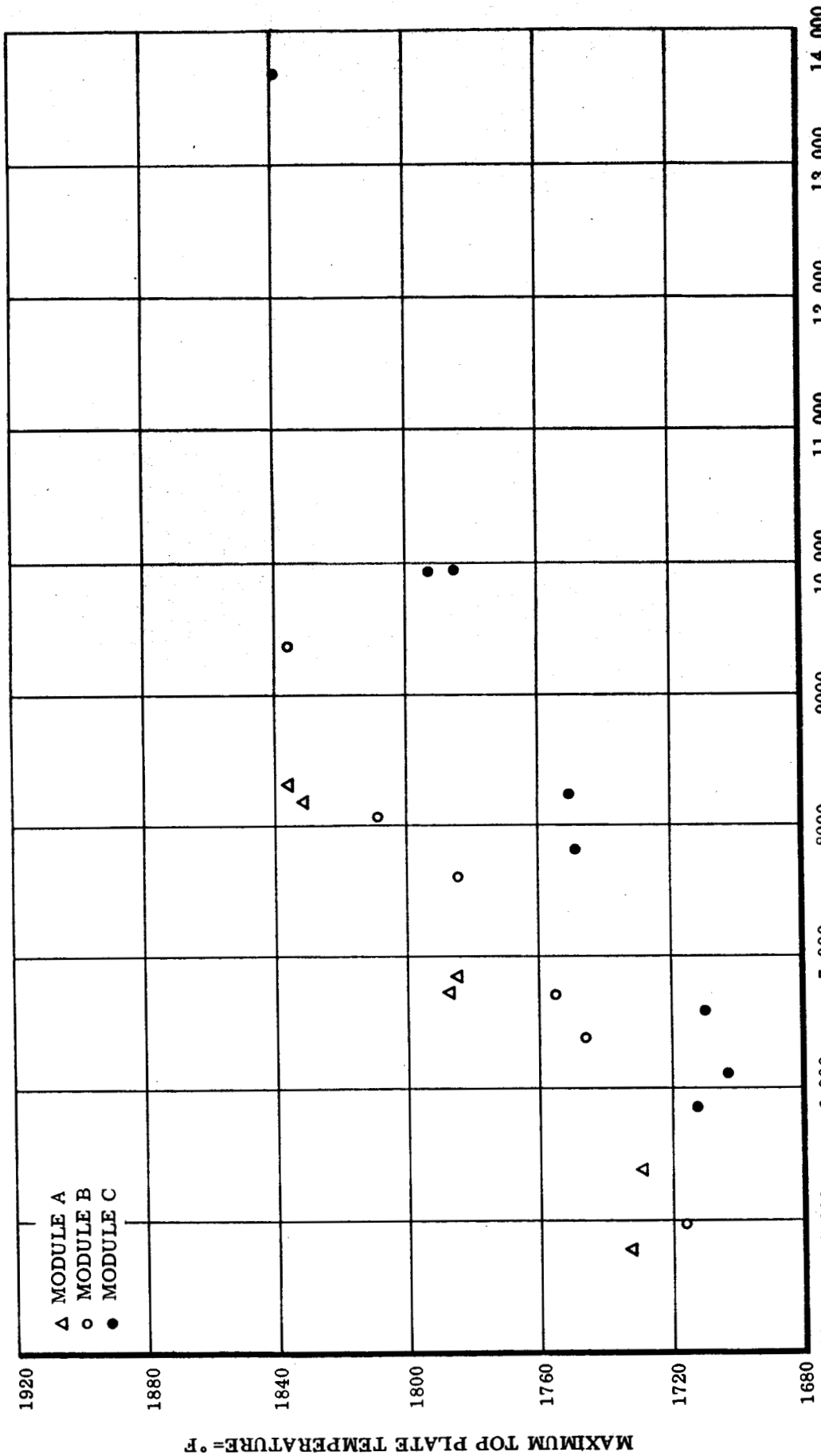

FIGURE 10

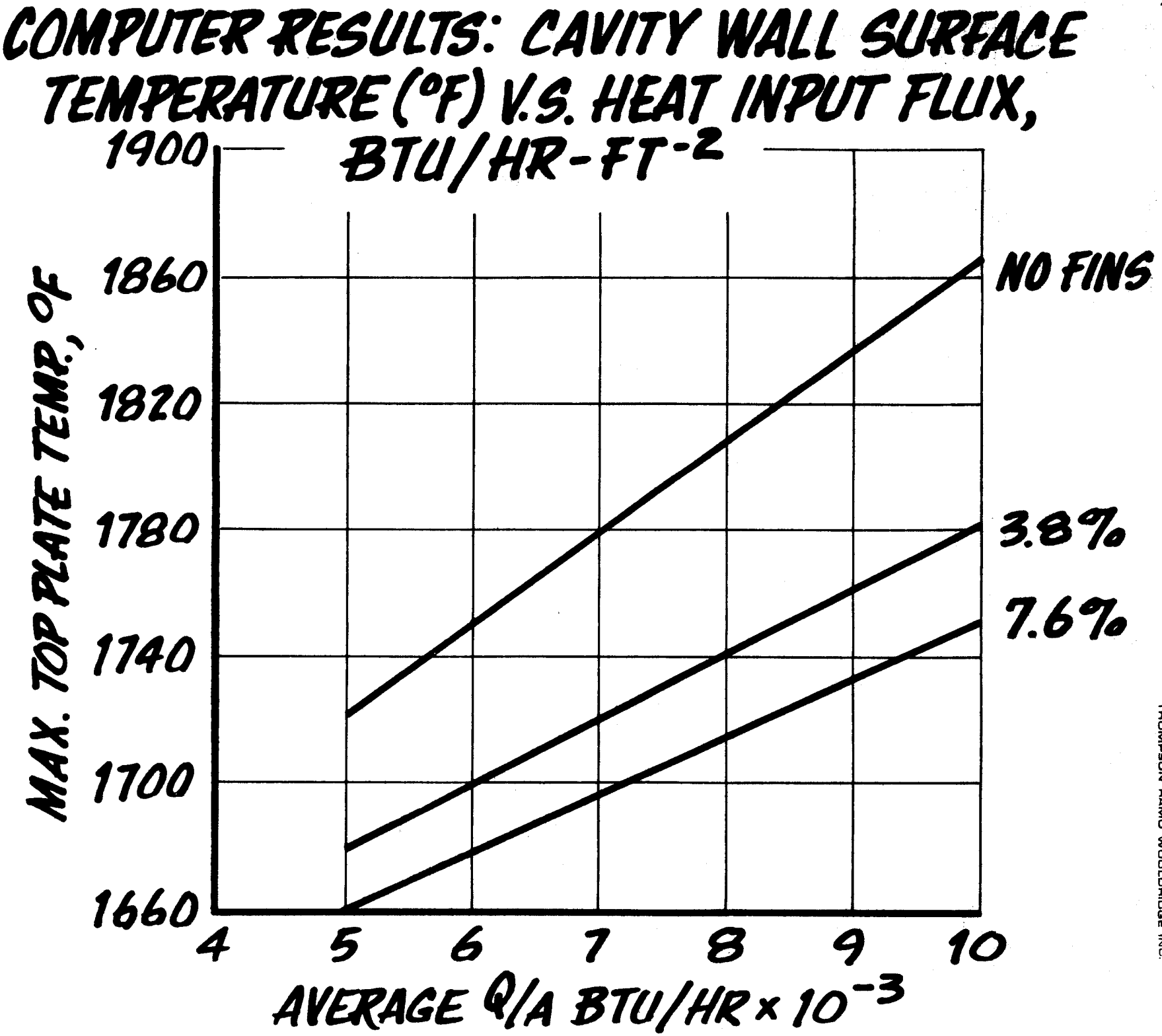

FIGURE 11

TRW ELECTROMECHANICAL DIVISION
THOMPSON RAMO WOOLDRIDGE INC.

PROJECT SCHEDULE, TASK IV, TWO PERCENT GAS PRESSURE DROP RECEIVER/HEAT STORAGE DESIGN

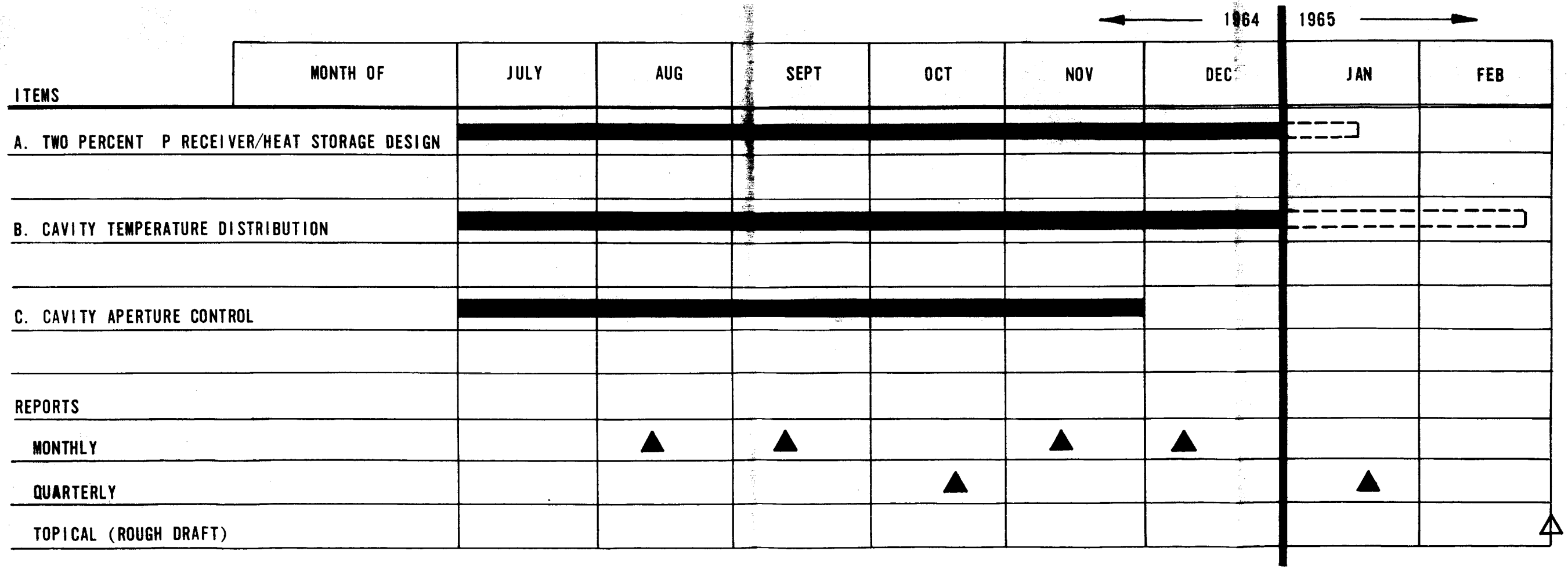

FIGURE 12

30 TUBE RECEIVER BRAYTON CYCLE

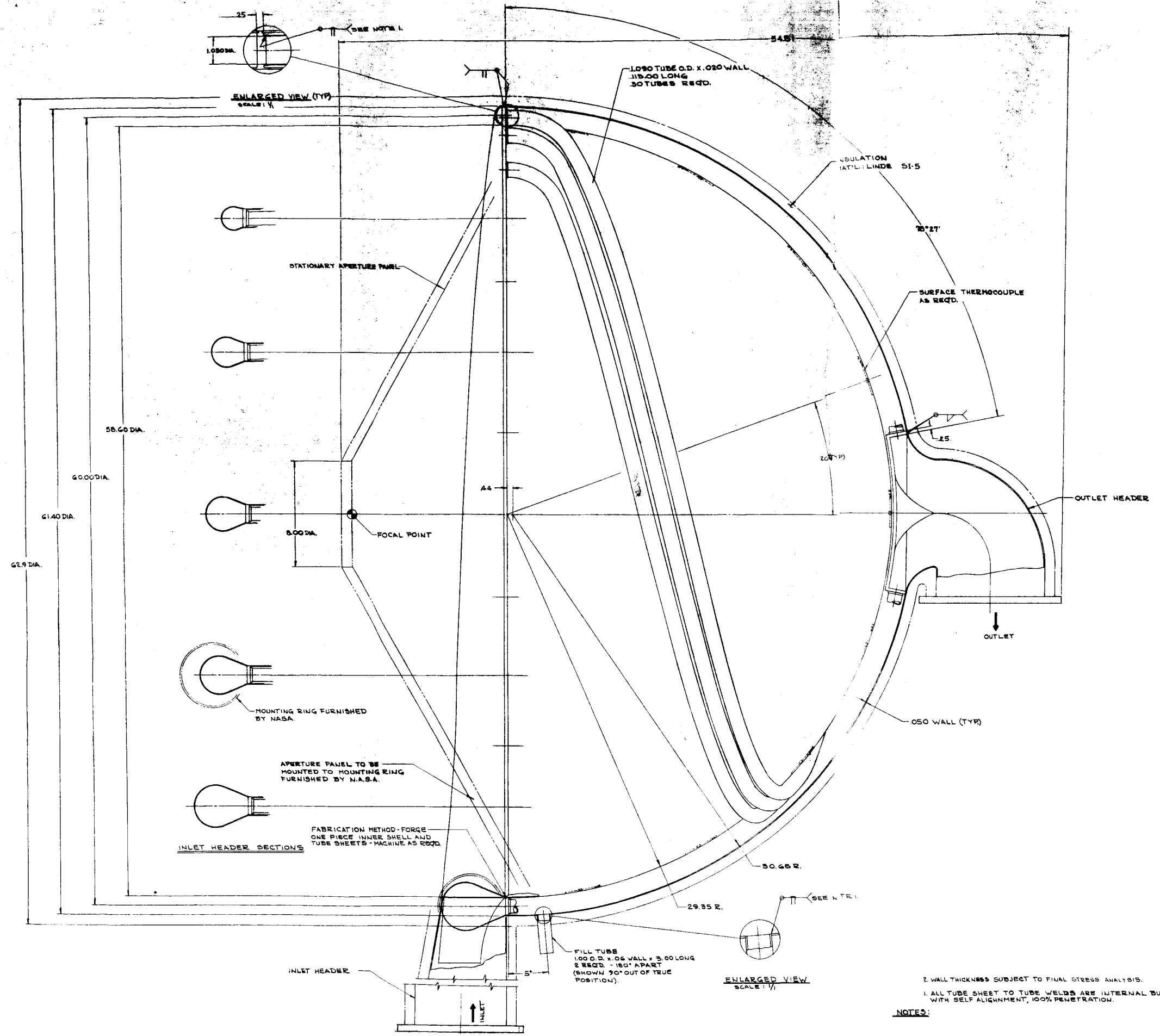

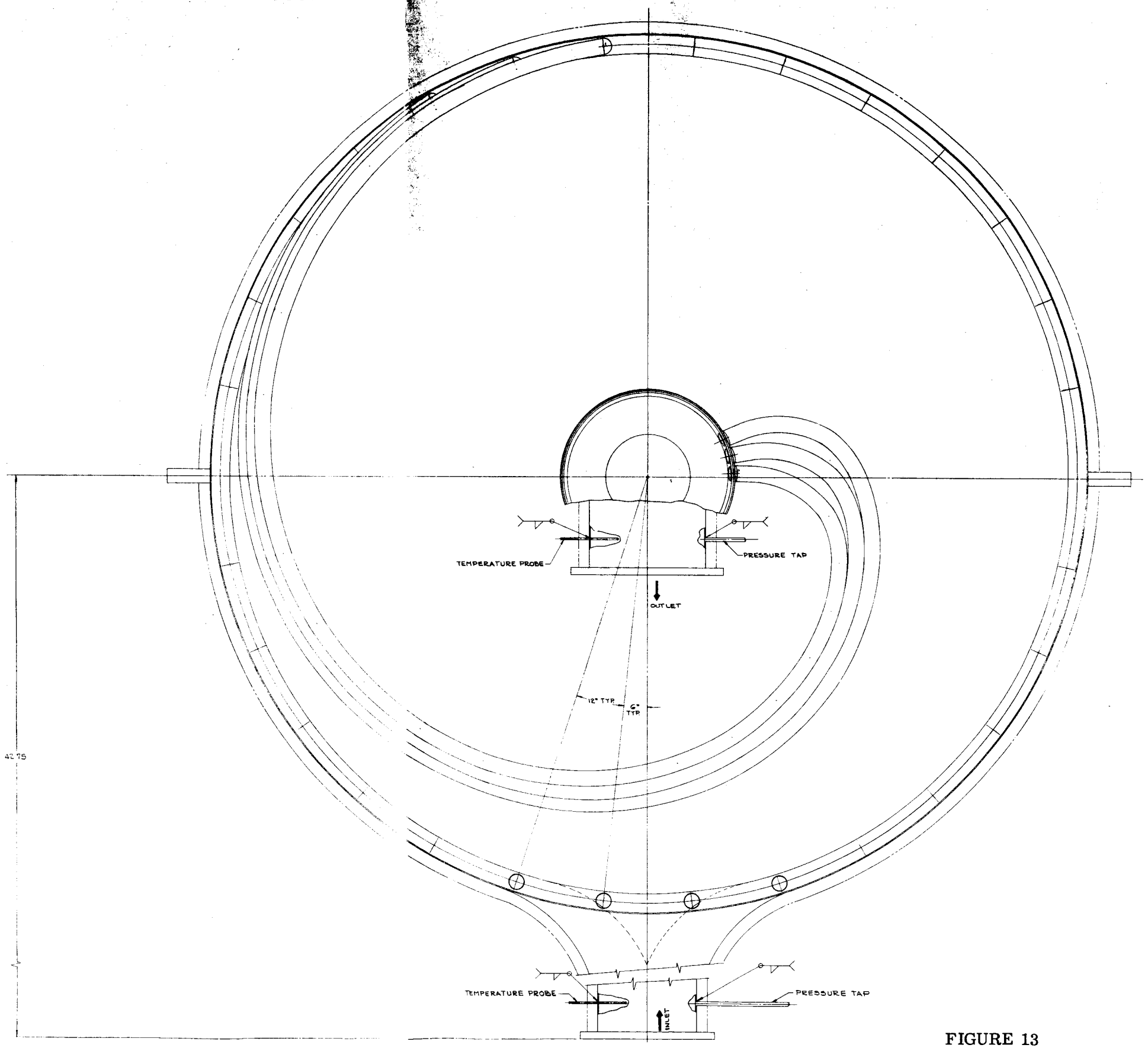

FIGURE 13

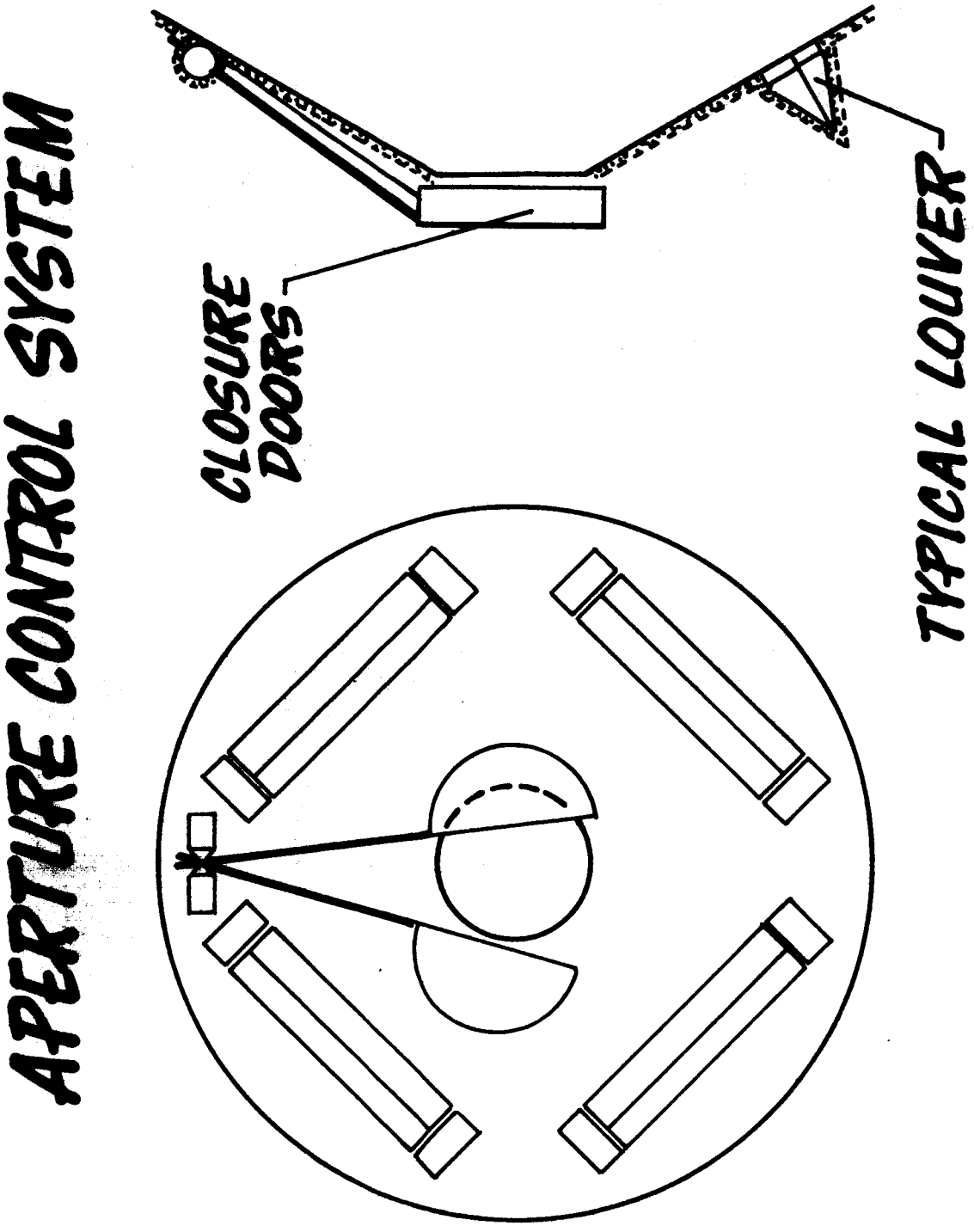

FIGURE 14

CAVITY RECEIVER PERFORMANCE ANALYSIS SCHEMATIC

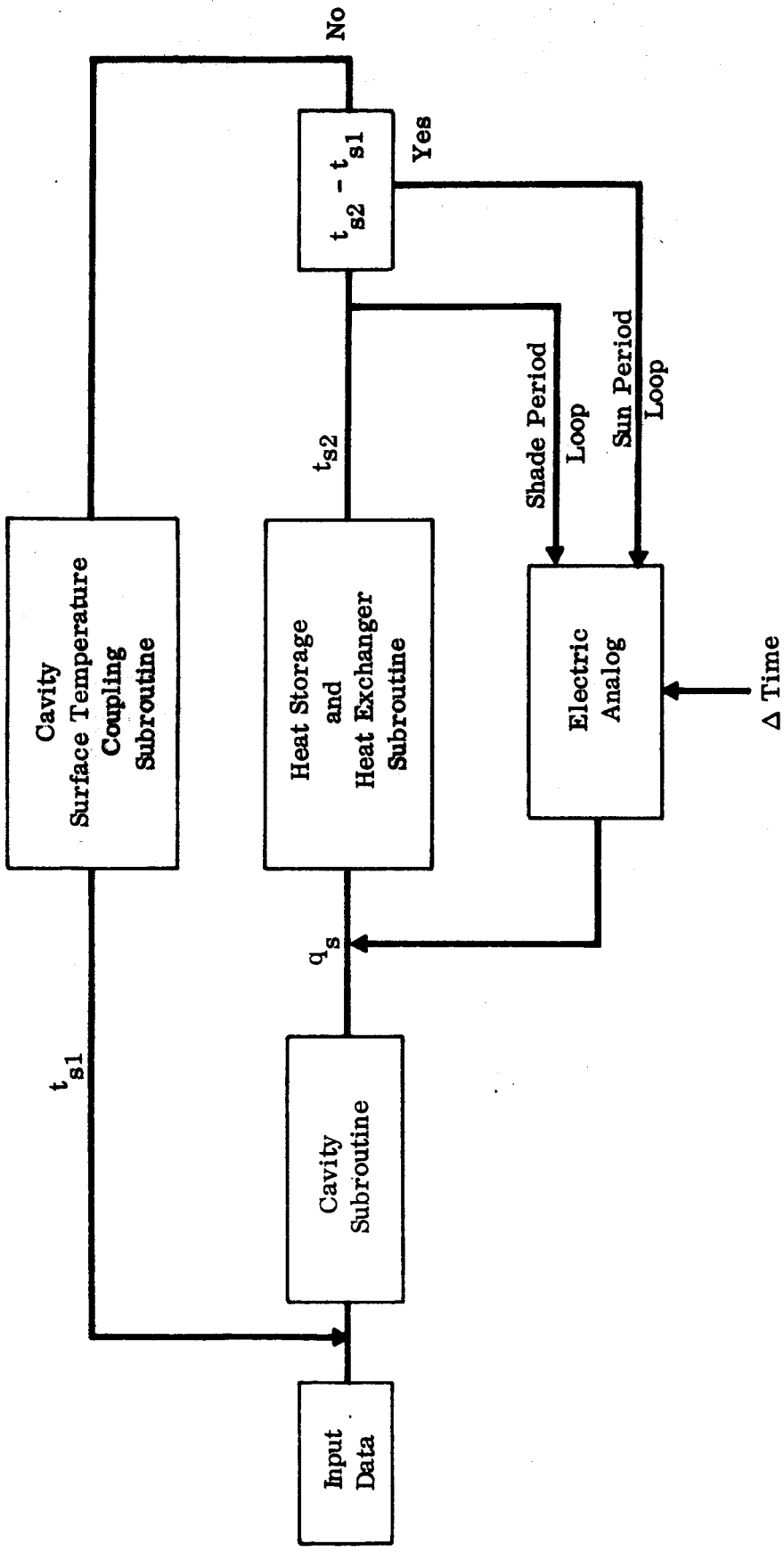

FIGURE 15

ELECTRIC ANALOG SIMULATION HEAT ADDITION

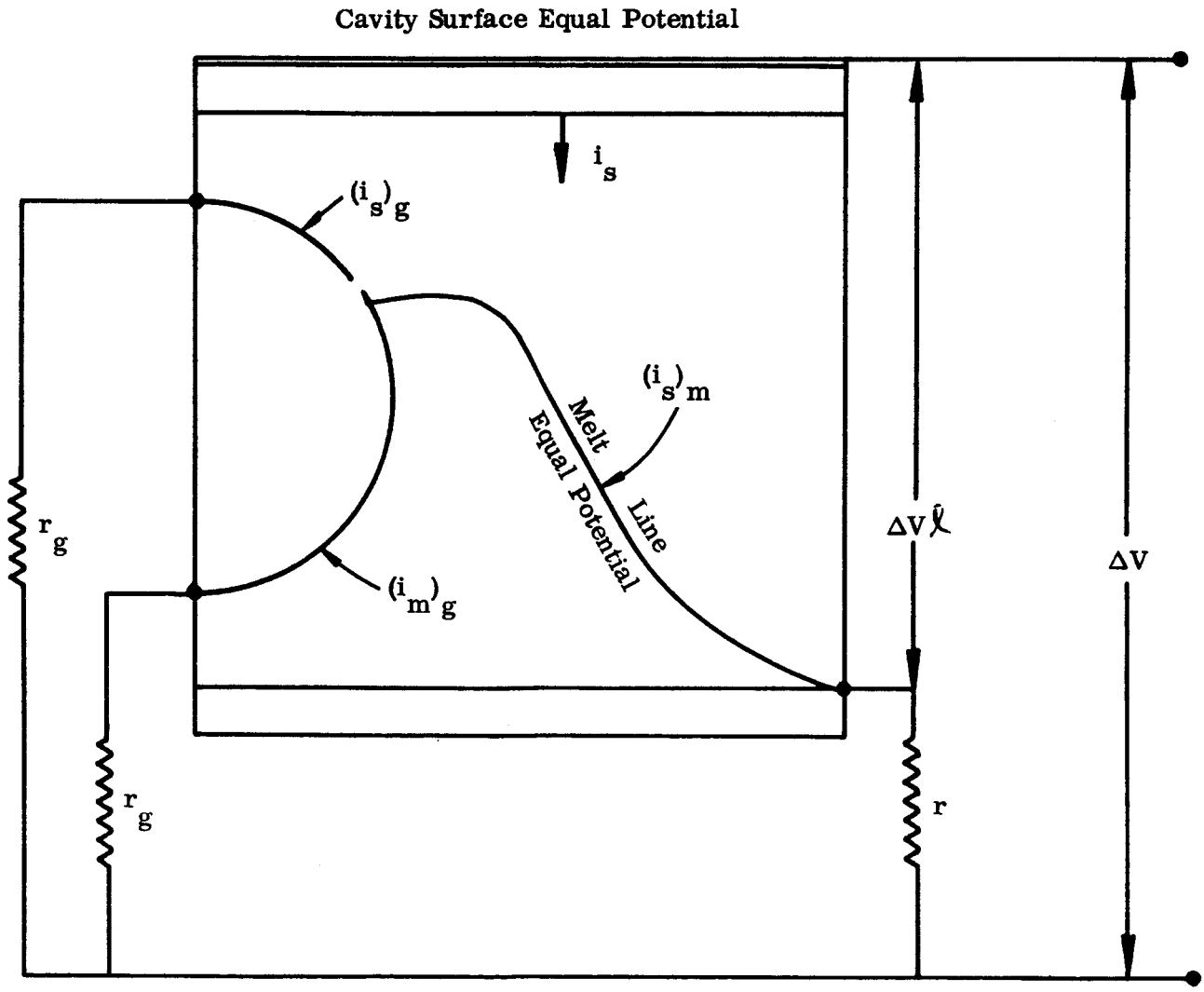

FIGURE 16

GEOMETRICAL RESISTANCE CHARACTERISTICS
IN HEAT TRANSFER THROUGH L. F. STORAGE

$T_{CAVITY\ WALL}$ = 1580°F
$T_{ARGON\ SINK}$ = 1017°F

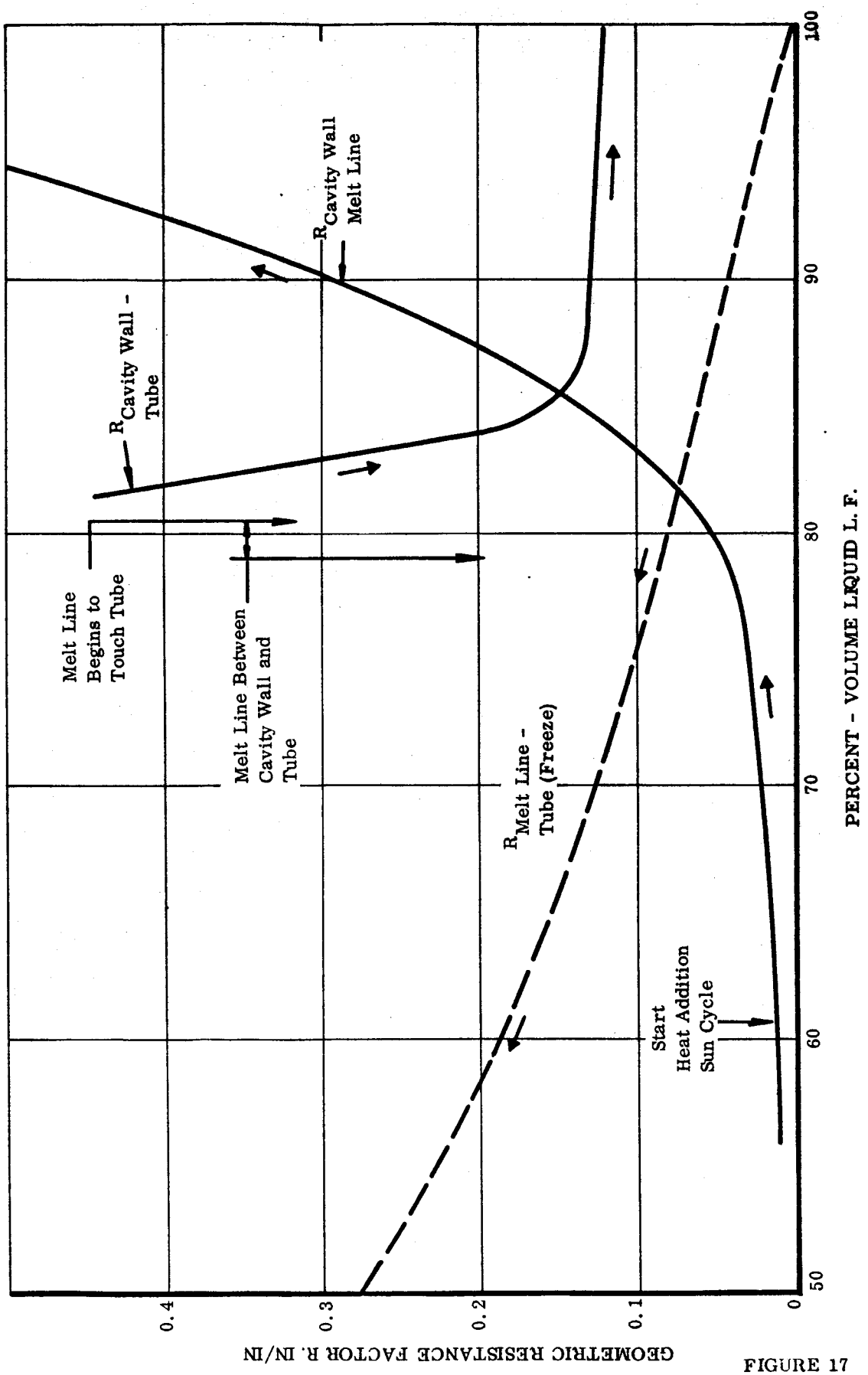

FIGURE 17

DISTRIBUTION LIST

Copy No.

1 National Aeronautics & Space Administration
1512 H Street, Northweat
Washington 25, D. C.
Attention: Walter Scott (RP)

2 National Aeronautics & Space Administration
1512 H Street, Northwest
Washington 25, D. C.
Attention: Herbert Rochen (RNEP)

3 National Aeronautics & Space Administration
1512 H Street, Northwest
Washington 25, D. C.
Attention: George Deutsch

4 Lewis Research Center
National Aeronautics & Space Administration
21000 Brookpark Road
Cleveland 35, Ohio
Attention: Dr. Bernard Lubarsky

5 Lewis Research Center
National Aeronautics & Space Administration
21000 Brookpark Road
Cleveland 35, Ohio
Attention: R. L. Cummings

6 Lewis Research Center
National Aeronautics & Space Administration
21000 Brookpark Road
Cleveland 35, Ohio
Attention: Dr. Louis Rosenblum

7 Lewis Research Center
National Aeronautics & Space Administration
21000 Brookpark Road
Cleveland 35, Ohio
Attention: D. C. Guentert

Copy No.

8 — Lewis Research Center
National Aeronautics & Space Administration
21000 Brookpark Road
Cleveland 35, Ohio
Attention: J. A. Heller (86-1)

9, 10 — Lewis Research Center
National Aeronautics & Space Administration
21000 Brookpark Road
Cleveland 35, Ohio
Attention: J. A. Milko (86-1)

11 — Lewis Research Center
National Aeronautics & Space Administration
21000 Brookpark Road
Cleveland 35, Ohio
Attention: T. A. Moss (MS 86-5)

12 — Lewis Research Center
National Aeronautics & Space Administration
21000 Brookpark Road
Cleveland 35, Ohio
Attention: R. P. Krebs

13 — Lewis Research Center
National Aeronautics & Space Administration
21000 Brookpark Road
Cleveland 35, Ohio
Attention: J. E. Dilley

14 — Lewis Research Center
National Aeronautics & Space Administration
21000 Brookpark Road
Cleveland 35, Ohio
Attention: N. T. Musial

15 — Ames Research Center
National Aeronautics & Space Administration
Moffett Field, California
Attention: Librarian

16 — Goddard Space Flight Center
National Aeronautics & Space Administration
Washington 25, D. C.
Attention: Librarian

Copy No.

17 Langley Research Center
National Aeronautics & Space Administration
Hampton, Virginia
Attention: Librarian

18 Marshall Space Flight Center
National Aeronautics & Space Administration
Huntsville, Alabama
Attention: Librarian

19 Lewis Research Center
National Aeronautics & Space Administration
21000 Brookpark Road
Cleveland 35, Ohio
Attention: Librarian

20 National Bureau of Standards
Washington 25, D. C.
Attention: Librarian

21 U. S. Naval Research Laboratory
Washington 25, D. C.
Attention: Librarian

22 Jet Propulsion Laboratory
California Institute of Technology
Pasadena, California
Attention: Librarian

23 Air Force Systems Command
Aeronautical Systems Division
Wright Patterson Air Force Base, Ohio
Attention: G. Thompson

24 Air Force Systems Command
Aeronautical Systems Division
Wright Patterson Air Force Base, Ohio
Attention: Librarian

25 U. S. Atomic Energy Commission
Technical Reports Library
Washington 25, D. C.
Attention: Librarian

Copy No.

26 U. S. Atomic Energy Commission
Technical Information Extension
P. O. Box 62
Oak Ridge, Tennessee
Attention: Librarian

27 Union Carbide Nuclear Company
X-10 Laboratory
P. O. Box X
Oak Ridge, Tennessee
Attention: J. H. DeVan

28 General Electric Company
Space Power and Propulsion Section
Bldg. 700, Mail Drop N-20
Cincinnati, Ohio 45215
Attention: E. E. Hoffman

29 Union Carbide Nuclear Company
X-10 Laboratory
P. O. Box X
Oak Ridge, Tennessee
Attention: Librarian

30 Argonne National Laboratories
Lemont, Illinois
Attention: Librarian

31 Battelle Memorial Institute
505 King Avenue
Columbus, Ohio
Attention: Librarian

32 Armour Research Foundation
Technical Center
Chicago, Illinois
Attention: Librarian

33 AiResearch Manufacturing Division
The Garrett Corporation
Phoenix, Arizona
Attention: Librarian

Copy No.

34 Allison Division
General Motors Corporation
Indianapolis 6, Indiana
Attention: Librarian

35 General Electric Company
Missile & Space Vehicle Department
3198 Chestnut Street
Philadelphia 4, Pennsylvania
Attention: Librarian

36 Electro-Optical Systems, Inc.
125 N. Vinedo Avenue
Pasadena, California
Attention: Librarian

37 Space Technology Laboratories
P. O. Box 95001
Los Angeles 45, California
Attention: Librarian

38 Sunstrand Denver
2480 West 70 Avenue
Denver 21, Colorado
Attention: Librarian

39 Aerojet General Corporation
Azusa, California
Attention: Librarian

40 Pratt & Whitney Aircraft
400 Main Street
East Hartford, Connecticut
Attention: Librarian

41 Pratt & Whitney Aircraft
CANEL
Middletown, Connecticut
Attention: Librarian

42 General Electric Company
FPLD
Cincinnati, Ohio
Attention: Librarian

Copy No.

43	MSA Research Corporation Callery, Pennsylvania Attention: Librarian
44	Lithium Corporation of America Inc. Bessemer City, North Carolina Attention: Librarian
45	Foote Mineral Company Philadelphia, Pennsylvania Attention: Librarian
46	Bendix Corporation Southfield, Michigan Attention: G. T. Burton
47	Department of Engineering University of California Los Angeles, California Attention: Librarian
48	Manned Space Center National Aeronautics & Space Administration Houston, Texas Attention: Librarian
49, 50 plus reproducible	National Aeronautics & Space Administration Scientific and Technical Information Center Box 5700 Bethesda 14, Maryland Attention: NASA Representative
51	Lewis Research Center National Aeronautics & Space Administration 21000 Brookpark Road Cleveland 35, Ohio Attention: W. W. Hu